THE JOURNAL OF PHYSICAL CHEMISTRY B LETTERS

**2006,** *110,* 8544−8547
Published on Web 04/12/2006

# Calculation of Activation Energies for Transport and Recombination in Mesoporous $TiO_2$/Dye/Electrolyte Films—Taking into Account Surface Charge Shifts with Temperature

**Brian C. O'Regan* and James R. Durrant**

*Department of Chemistry, Imperial College London, Exhibition Rd., London SW7 2AZ*

*Received: February 15, 2006; In Final Form: March 17, 2006*

Transient photovoltage and photocurrent measurements have been employed to determine the recombination and transport kinetics in operating dye-sensitized photovoltaic cells as a function of potential and temperature. Photocurrent transients have been taken at the open circuit potential, as opposed to the standard measurement at short circuit. Kinetic results have been used to calculate the activation energy as function of the Fermi level position in the $TiO_2$. In the calculation of activation energies, we have explicitly taken into account the temperature dependence of the offset between the electrolyte redox potential and the conduction band edge. This new method gives activation energies that decrease linearly as the Fermi level position moves toward the conduction band edge, as expected, but not found in previous studies. The results are consistent with the presence of a distribution of traps below the $TiO_2$ conduction band, the detrapping from which limits both the transport and the recombination of electrons.

## Introduction

Dye-sensitized photovoltaic (PV) cells are interesting devices both in their own right and as test beds for examination of models of nanostructured electrodes. Dye-sensitized PV cells consist of a 3−15-$\mu$m-thick mesoporous layer of $TiO_2$ nanoparticles (the electron conductor) perfused with an electrolyte or a solid hole conductor. During successful device operation, counter currents of photogenerated electrons and holes flow in their respective conductors with minimal losses to interfacial recombination, despite the short separation distances and large surface area of contact. Successful operation, however, is limited to a very small selection of electrolytes and hole conductors, with the $I^-/I_3^-$ electrolyte having double the efficiency of the nearest competitor. It is clear that a full model of transport and recombination is vitally important to further optimization of these devices and also as a general contribution to nanoelectronics.

The kinetics of electron transport and electron recombination with the electrolyte have been investigated as a function of the Fermi level potential in the $TiO_2$, or light intensity, since 1990.[1−8] These studies have all found exponentially increasing transport and recombination rates as potential, or light intensity, was increased. Most studies have concurred that both processes are limited by thermally activated detrapping of electrons in the $TiO_2$.[1] The traps are thought to occur as an exponentially decreasing tail of states below the conduction band edge. As the applied potential, or $V_{oc}$, increases, the Fermi level in the $TiO_2$ moves toward the conduction band and electron traps below the Fermi level are filled. Under the assumption that both transport and recombination require thermal detrapping of electrons from near the Fermi level, we would expect an activation energy for both that is similar to the distance from the Fermi level to the conduction band edge (or mobility edge). At low potentials, these activation energies should be quite large ($\geq$400 mV) and should decrease by 50 mV for every 50 mV increase in the potential. Note that this relationship will also hold if the limiting step in recombination is detrapping from near the Fermi level to a set of surface states of defined energy with respect to the conduction band.

It is thus important to obtain experimental data on the activation energy of these processes, such as temperature-dependent kinetic studies. For the recombination reaction, we present the first such data herein. Two temperature-dependent studies of electron transport at short circuit have been recently published.[9,10] In these studies, the calculated activation energies were small and not dependent on the light intensity or charge density, in contrast to the expectations of the detrapping model discussed above.

One factor not addressed in the aforementioned publications is that the surface charge at a semiconductor/electrolyte interface is temperature-dependent. This dependence arises from the changing adsorption equilibrium constants for the ions in the electrolyte. The surface charge controls the electric field at the interface between the semiconductor and the electrolyte/hole conductor. In the case of dye-sensitized cells, the surface electric field controls the potential difference between the $TiO_2$ conduction band (and the electron trap states under it) and the redox potential of the electrolyte. For example, the surface potential of $TiO_2$ in water solution is known to vary by ~60 mV between 0 and 70 °C.[11] In addition, the redox potential of the electrolyte can change with temperature. Together, these effects create a changing offset between the potential of the electrolyte and the band and traps states in the $TiO_2$. Since potential measurements in these kinds of experiments are referenced to the electrolyte potential, or to a reference electrode therein, a changing offset between the reference potential and the states in the $TiO_2$ cannot be ignored in the analysis. We show a simple method for including offset potential changes in the calculation of activation energies and detail the profound effect this has on the conclusions reached.

10.1021/jp060979w CCC: $33.50 

## Methods

Dye-sensitized photovoltaic cells were made with standard methods, using the N3 dye.[12,13] The sample used for Figures 1−5 had a $TiCl_4$ treatment.[13] The electrolyte was based on acetonitrile with 0.6 M proplymethylimidazolium iodide, 0.1 M LiI, and 0.5 M *tert*-butylpyridine. A lithium-free electrolyte was also tested, as was a cell without $TiCl_4$ treatment. Temperature control was provided by a water-cooled/heated plate attached to the cell, monitored by thermistors at several points. Photovoltage and photocurrent transients were measured using a variable white bias light and a low-intensity pulse light from an array of red LEDs. The equipment and analysis have been previously described.[14]

Photovoltage transients were measured at open circuit potential. The transient voltage peak was kept at <5 mV. Recombination rate constants were found from the single-exponential voltage decays. Capacitance and differential density of states (DOS) at each $V_{oc}$ were calculated from the photovoltage transients as previously published.[14] Briefly, we calculate the capacitance as $C = \Delta Q/\Delta V$, using the peak of the photovoltage transient as $\Delta V$ and the photoinjected charge as $\Delta Q$. The photoinjected charge is found by integrating the short circuit photocurrent transient caused by a pulse of the same intensity. This is a good estimate of the injected charge in dye-sensitized electrolyte cells where recombination losses during transport are small. Because the high concentration of iodine and iodide fixes the potential of the electrolyte, the shift in the measured voltage corresponds to a shift of the Fermi level in the $TiO_2$. Thus, the $TiO_2$ DOS at a given $V_{oc}$ can be calculated directly from the capacitance, if the thickness of the film and the porosity are known.

Charge transport was measured at the open circuit potential ($V_{oc}$) by the following method. Cells were placed under bias light, connected to a voltage source. The applied voltage was set equal to the $V_{oc}$ established by the bias light. Thus, the cell is in the same condition as "open circuit" for that light intensity, and no current flows through the external circuit. A pulse of light is applied. Pulse intensities were ~5 times lower than those used for the photovoltage transients. The pulse light causes a small increase in the Fermi level in the $TiO_2$, which at open circuit would cause an increase in the measured potential. However, because the applied potential at the external electrodes is fixed at the "pre-pulse" $V_{oc}$, the increase in the Fermi level causes a current to flow through the external circuit until the "pre-pulse" condition is reestablished. Because the transport rate at $V_{oc}$ in these cells is much faster than the recombination rate, the resulting photocurrent transient contains most of the injected electrons and is a good measure of electron transport at $V_{oc}$ (Figure 1b inset). To extract charge transport times, the photocurrent transients were integrated to photocharge transients. This avoids errors in fitting when small peaks are present at the start of the photocurrent transient. Charge transport times ("extraction times") were found by fitting an exponential to the last $^2/_3$ of the integrated photocurrent transients.

## Results and Discussion

Figure 1a shows typical photovoltage transients for a range of $V_{oc}$ values at room temperature. The typical strong decrease in recombination lifetime occurs with increasing $V_{oc}$. Figure 1b shows a set of photovoltage transients measured at a constant $V_{oc}$ and varying temperature. To hold constant $V_{oc}$, the bias light was varied. A strong decrease in recombination lifetime occurs with increasing temperature. Figure 1b inset shows a photovoltage transient and an integrated photocurrent transient both

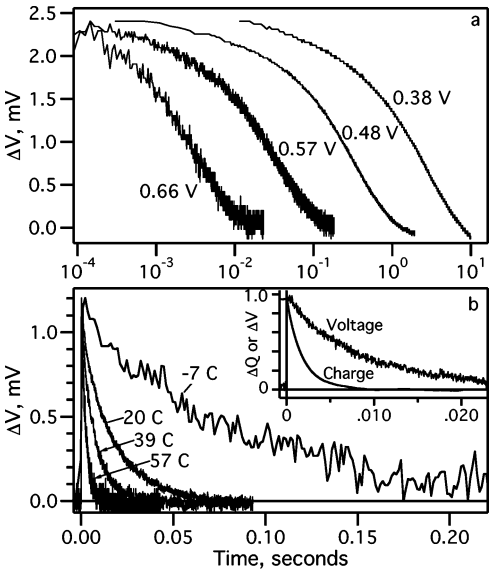


**Figure 1.** (a) Typical normalized photovoltage transients at open circuit for a range of bias light-induced $V_{oc}$'s. $T = 20$ C. All transient peaks were ≤4 mV. (b) Normalized photovoltage decays at constant $V_{oc} = 0.6$ V for various temperatures. Inset: Comparison of the transient photovoltage decay and the integrated "photocurrent transient at $V_{oc}$" at $V_{oc} = 0.55$ V. $T = 20$ C.

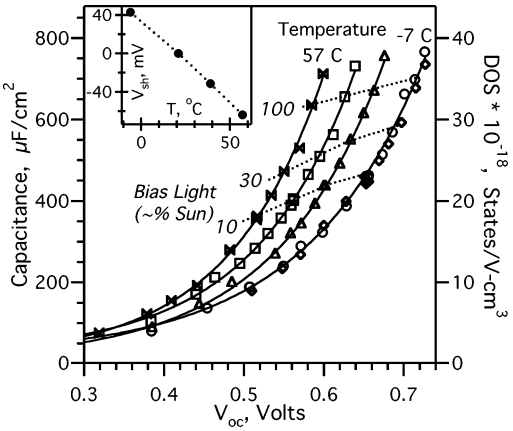


**Figure 2.** Capacitance/density of states vs voltage ($V_{oc}$) curves for a $TiO_2$/dye/electrolyte interface at temperatures −7, 20, 39, and 57 °C. Fit lines (solid) are single exponentials. Dotted lines connect points on the DOS curves that correspond to a given bias light intensity, labeled with the fraction of "one sun" (~100 mW/cm²). Inset: Lateral shift in the DOS curves as a function of temperature, relative to the DOS at 20 °C.

measured at a the same $V_{oc}$. In the example shown, the recombination lifetime is ten times longer than the "extraction" lifetime, thus 90% of the photoinjected electrons are collected during the photocurrent transient. All samples had collection efficiencies at least this large.

Photovoltage and photocurrent transients were measured at $V_{oc}$ for twelve bias light levels and four temperatures. Figure 2 shows the calculated capacitance and DOS vs $V_{oc}$ for one sample. It is clear that the DOS distribution has shifted to smaller values of $V_{oc}$ (toward the $I^-/I_3^-$ potential) with increasing temperature. The direction of the shift in Figure 2 corresponds to an increase in the net positive charge at the $TiO_2$ surface and/or a negative movement of the redox potential of the $I^-/I_3^-$ couple. Because of the lack of thermodynamic data for $I^-/I_3^-$ in acetonitrile, we cannot state which effect predominates. Since there is no significant change in the shape of the DOS distribution with temperature, we assume that the relatively small

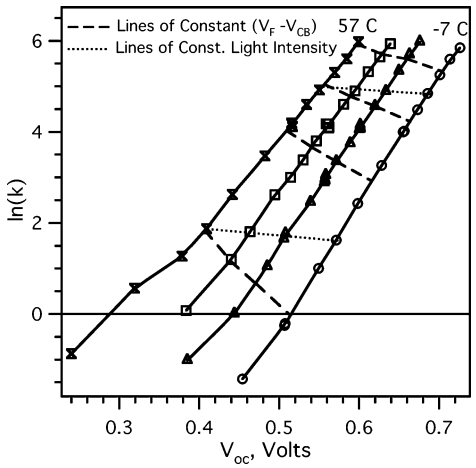


**Figure 3.** Recombination rate constant ($k_r$) vs voltage ($V_{oc}$) data measured for a $TiO_2$/dye/electrolyte interface at temperatures −7, 20, 39, and 57 °C. Dashed lines connect $k_r$ values corresponding to constant $V_F-V_{CB}$ (see text). Dotted lines connect $k_r$ values corresponding to constant light levels.

changes in temperature do not affect the number of traps at a given depth below the conduction band. (For example, they should not affect the equilibrium oxygen vacancy concentration.) Thus, a constant DOS in Figure 2 corresponds to a given position of the Fermi level relative to the conduction band edge ($V_F-V_{CB}$) at all temperatures. We can determine the shift of the conduction band, relative to $I^-/I_3^-$, directly from the lateral shift of the DOS curve, measured at constant DOS. For this sample, the band edge at 57, 39, and −7 °C has moved −63, −31.5, and +45 mV respectively, relative to that at 20 °C.

Figure 3 shows the measured recombination rate constants ($k_r$) for the same sample, as function of $V_{oc}$ and temperature. To determine an Arrhenius activation energy ($E_a$), one needs to plot ln($k_r$) vs 1/$T$, but the question arises which $k_r$ from each temperature is appropriate. If the recombination rate is limited by detrapping from traps near the Fermi level to the conduction band (or any other states with a fixed energy relative to the conduction band), then the $E_a$ can only be found by comparing rate constants that were measured when the Fermi level was at a constant depth below the conduction band. Note that this is not the same as constant $V_{oc}$ or constant light level. $k_r$ at constant $V_F-V_{CB}$ can be found with the following procedure. Chose an arbitrary open circuit voltage, $V$. From the 20 °C data, find the $k_r$ that corresponds to this $V$ and call this $k_{r20}(V)$. Then, from the 39 °C data, find $k_{r39}$ that corresponds to $V + V_{sh39}$, where $V_{sh39}$ (= −0.0315) is the shift of the conduction band at 39 °C relative to that at 20 °C. Continue for the remaining temperatures. In Figure 3, several dashed lines are shown connecting sets of $k_r$ points with constant $V_F-V_{CB}$. The sets are each {$k_{r57}(V - 0.063)$, $k_{r39}(V - 0.0315)$, $k_{r20}(V)$, $k_{r-7}(V + 0.044)$} for different $V$. Figure 4 shows five sets of "$k_r$ at constant $V_F-V_{CB}$" points, plotted as ln($k_r$) vs 1/$T$. The plots are reasonably linear, and thus, the Arrhenius equation can be used to derive activation energies. Figure 5 shows the calculated activation energies, plotted with respect to the $V_{oc}$ at 20 °C. This voltage scale is employed as it requires no assumptions about the absolute value of $V_{cb}$, which is unknown. On the upper axis, a *possible* $V_F-V_{CB}$ scale is given, assuming the conduction band edge at 20 °C is 900 mV negative of the $I^-/I_3^-$ redox potential.[8] The most important observation from Figure 5 is that $E_a$ decreases linearly with increasing Fermi level position with a slope near −1. This is entirely consistent with the hypothesis that detrapping from traps at the Fermi level is the limiting step in recombination. Figure 5 also shows $E_a$ vs $V_{oc}$ for a cell

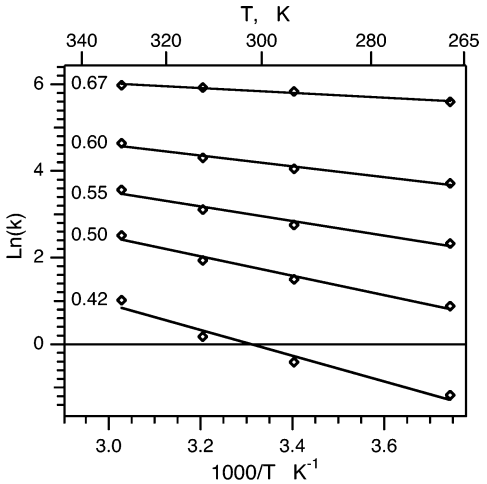


**Figure 4.** Arrhenius plot of recombination rate constants for four temperatures and five values of $V_F-V_{CB}$. Sets of points of constant $V_F-V_{CB}$ are labeled with the corresponding $V_{oc}$ at 20 °C.

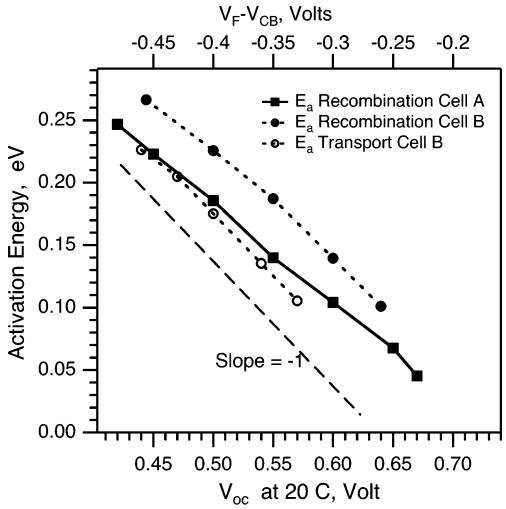


**Figure 5.** Arrhenius activation energies vs $V_{oc}$ and vs $V_F-V_{CB}$ assuming $V_{CB}$ = 0.9 V vs $I^-/I_3^-$ (top axis). Solid squares are the activation energy for recombination for the sample shown in Figures 1−4. Solid circles are for a similar sample which had no $TiCl_4$ treatment. Activation energies for transport at $V_{oc}$ are also shown for this sample (open circles).

without the $TiCl_4$ treatment; the same trend is evident. We have found a similar trend in a cell without lithium in the electrolyte.

A similar analysis can be applied to transport measurements made at $V_{oc}$. Since the Fermi level is essentially flat during the measurement, the DOS values in Figure 2 are applicable. The same procedure is used to find ln($k_t$) vs 1/$T$, at constant $V_F-V_{CB}$, and to derive activation energies. One set of results is plotted in Figure 5. The activation energy for transport also decreases with increasing potential, with slope of ∼−1, indicating that detrapping from the Fermi level is controlling the transport at $V_{oc}$. This result differs from those derived from photocurrent measurements performed at short circuit where the calculated $E_a$ varied only slightly with charge density or light intensity.[9,10] However, when measuring photocurrent at short circuit, the charge density and Fermi level vary strongly across the thickness of the film. It may not be obvious where in the film the limiting steps for transport are occurring and to what extent changes in total charge density are reflected at that point. (We also note that neither publication corrected for the temperature dependence of the reference electrode used.) In contrast, the measurement of photocurrent transients at $V_{oc}$ has the

advantage that the Fermi level, charge density, and effective diffusion constant are all constant across the thickness of the $TiO_2$ film. This provides conditions which allow a more robust comparison of $E_a$ and Fermi level position. Further description of charge transport measurements at $V_{oc}$ will be provided elsewhere (in preparation).

One striking feature in Figure 5 is that the activation energy for transport is 60 mV smaller than that for recombination in the same sample. This is close to the binding energy of the electron polaron in $TiO_2$.[15] In principle, transport will require detrapping to the polaron state, but recombination might involve an extra energy cost to reach the surface, where a lower polarization stabilization may apply. It is also interesting to note that the trends in Figure 5 would appear to give activation energies that reach zero when the Fermi level is still 150 mV below the conduction band edge (see the top axis) Although this could be corrected by placing the conduction band 150 mV closer to the $I^-/I_3^-$ level, this would be lead to another contradiction. If the Fermi level is within 60 mV of the conduction band, and the DOS at the edge of the conduction band is on the order of $10^{21}/cm^3$, then the density of electrons in the conduction band has to be $\sim 10^{20}/cm^3$. This number is $\sim$20 times larger than the actual density of electrons in the films ($5 \times 10^{18}/cm^3$) measured by integrating the DOS curves and by charge extraction.[5] This seems to indicate that the required activation energies are not to the "conduction band edge", but rather to some surface states, and/or a mobility edge, located below the conduction band. This may be related to defect states or again to the polaron nature of the electron in $TiO_2$.

Many studies of recombination and transport in dye-sensitized cells have been carried out as a function of incident light intensity. It might be assumed that comparing $\ln(k)$ vs $1/T$ at constant illumination intensity would allow calculation of $E_a$. In fact, this analysis gives erroneously small activation barriers and misses the dependence of $E_a$ on Fermi level position. This can be seen in Figure 3, where lines of constant light intensity are shown connecting sets of $\ln(k)$ data. These lines are almost flat, showing little increase in rate constant for increasing temperature. The reason for this is shown in Figure 2 where lines of constant light intensity are shown connecting points on the DOS vs $V_{oc}$ curves. As the temperature increases, the $V_{oc}$ for a given light level decreases by two effects. One is the downward movement of the band edge relative to $I^-/I_3^-$. The other is that the faster recombination rate results in a lower equilibrium concentration of electrons for a given light intensity, and thus a lower $V_F - V_{CB}$. Since $k$ depends on $V_F - V_{CB}$, plotting $\ln(k)$ vs $1/T$ using $\ln(k)$ values with differing $V_F - V_{CB}$ cannot give the correct activation energy.

Another possibility would be to compare $\ln(k_r)$ values at constant $V_{oc}$ rather than at constant $(V_F - V_{CB})$. This approach calculates activation energies $\sim$0.25 V larger than those shown in Figure 5, with approximately the same linear trend of $E_a$ with $V_{oc}$ (not shown). This would be the correct calculation of the activation energy if the recombination rate constant was controlled by the overpotential between the Fermi level in the $TiO_2$ and the iodine/iodide couple. The activation energy so calculated would correspond to the thermal energy needed to bring the empty acceptor orbital to the same potential as the Fermi level. Several characteristics of the data suggest this is not the correct model. Most importantly, using a Gaussian distribution for the potential of the acceptor states, it is not possible to reproduce the slope of $\ln(k_r)$ vs $V_{oc}$ seen in Figure 3 for *any* value of the reorganization energy. Second, using the standard quadratic model relating the shift in the acceptor state energy to the thermal energy of polarization of the solvent ($E_a = (V_{oc} - \lambda)^2/4\lambda$) does not reproduce the linear trend of $E_a$ with $V_{oc}$ seen.[16] Last, using the same equation, a reorganization energy ($\lambda$) of 2.7 eV is required to reproduce the calculated $E_a$ ($= 0.4$ V) at a $V_{oc}$ of 0.6 V. In sum, although it may be possible to construct a model where the rate constant is determined by the overpotential, it seems reasonable to stick with the "detrapping model" for the present.

In conclusion, under well-defined measurement conditions, and using a simple analysis, we find results consistent with the hypothesis that both transport and recombination are limited by detrapping from trap states distributed in energy below the conduction band.

**Acknowledgment.** We thank our colleagues at the Energy Research Centre of The Netherlands (ECN) for providing the dye-sensitized cells. Funding for this work was provided by the CEC project "Molycell" (no. 502783).

## References and Notes

(1) O'Regan, B.; Moser, J.; Anderson, M.; Gratzel, M. *J. Phys. Chem.* **1990**, *94*, 8720−8726.
(2) Schwarzburg, K.; Willig, F. *Appl. Phys. Lett* **1991**, *58*, 2520−2523.
(3) de Jongh, P. E.; Vanmaekelbergh, D. *Phys. Rev. Lett.* **1996**, *77*, 3427.
(4) Yan, S. G.; Hupp, J. T. *J. Phys. Chem.* **1996**, *100*, 6867−6870.
(5) Duffy, N. W.; Peter, L. M.; Rajapakse, R. M. G.; Wijayantha, K. G. U. *J. Phys. Chem. B* **2000**, *104*, 8916−8919.
(6) van de Lagemaat, J.; Park, N.-G.; Frank, A. J. *J. Phys. Chem. B* **2000**, *104*, 2044−2052.
(7) Fabregat-Santiago, F.; Garcia-Belmonte, G.; Bisquert, J.; Zaban, A.; Salvador, P. *J. Phys. Chem. B* **2002**, *106*, 334−339.
(8) O'Regan, B. C.; Lenzmann, F. *J. Phys. Chem. B* **2004**, *108*, 4342−4350.
(9) Boschloo, G.; Hagfeldt, A. *J. Phys. Chem. B* **2005**, *109*, 12093−12090.
(10) Kopidakis, N.; Benkstein, K. D.; van de Lagemaat, J.; Frank, A. J.; Yuan, Q.; Schiff, E. A. *Phys. Rev. B* **2006**, *73*, 045326.
(11) Fokkink, L. G. J.; de Keizer, A.; Lyklema, J. *J. Colloid Interface Sci.* **1989**, *127*, 116−131.
(12) Spath, M.; Sommeling, P. M.; van Roosmalen, J. A. M.; Smit, H. J. P.; van der Burg, N. P. G.; Mahieu, D. R.; Bakker, N. J.; Kroon, J. M. *Prog. Photovoltaics* **2003**, *11*, 207−220.
(13) Nazeeruddin, M. K.; Kay, A.; Rodicio, I.; Humphry-Baker, R.; Muller, E.; Liska, P.; Vlachopoulos, N.; Grätzel, M. *J. Am. Chem. Soc.* **1993**, *115*, 5, 6382−6390.
(14) O'Regan, B. C.; Scully, S.; Mayer, A. C.; Palomares, E.; Durrant, J. *J. Phys. Chem. B* **2005**, *109*, 4616−4623.
(15) Hendry, E.; Wang, F.; Shan, J.; Heinz, T. F.; Bonn, M. *Phys. Rev. B* **2004**, *60*, 81101.
(16) Morrison, S. R. *Electrochemistry at Semiconductor and Oxidized Metal Electrodes*; Plenum Press: New York, 1980.